# Hysteresis Behavior in the Sorption Equilibrium of Water in Anodes for Li-Ion Batteries

Jochen C. Eser,* Birthe Deichmann, Tobias Wirsching, Peter G. Weidler, Philip Scharfer, and Wilhelm Schabel

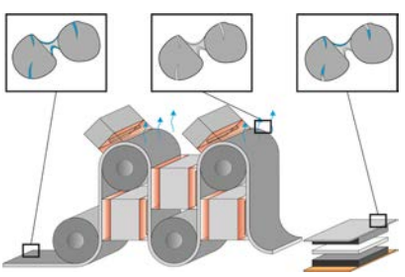

**ABSTRACT:** Hysteresis in the sorption equilibrium influences the production process of many multicomponent material systems. Electrodes for Li ion batteries consist of several materials, some of which exhibit hysteresis in their sorption equilibrium with water. The moisture content adsorbed and absorbed in the electrodes of the Li ion battery turned out to be an issue for its electrochemical performance and is reduced in the post drying process. During this process, hysteresis in the sorption equilibrium needs to be overcome in order to achieve a low residual moisture content of the electrode. Modeling the post drying process requires a description of the sorption equilibria of water in the components of the battery. This paper builds on previous research about the sorption equilibria and examines the hysteresis behavior of typical graphite anodes, with the active material graphite, carbon black as the conductive additive, and sodium carboxymethyl cellulose as well as styrene butadiene rubber as polymeric binders. Moreover, the mechanisms for the occurrence of hysteresis are presented, and how sorption equilibria during drying can be described is shown by applying models from the literature on the materials of battery electrodes. Theoretical deliberations on hysteresis mechanisms are validated, investigating graphite anodes of different material compositions and their materials.

## INTRODUCTION

In their process chain, electrodes for Li ion batteries are subjected to many individual process steps. An energy intensive process step is the post drying process,[1] which is often designed empirically and has hardly been addressed scientifically. In this process, moisture adsorbed and absorbed in the electrodes is removed to a certain amount. If the electrodes have reached their sorption equilibrium with dryer conditions, an unwanted remoistening takes place in the dry room during further cell processing. This remoistening happens as the electrodes aim for the sorption equilibrium with the gas phase in their vicinity. The activity of water $a_W$ in the electrode is given as a ratio of the partial pressure of water $p_W$ in the gas phase and the saturation vapor pressure at the temperature of the electrode $p_W^*$ ($T_{Electrode}$), resulting in $a_W = p_W/p_W^*$ ($T_{Electrode}$). It therefore adjusts according to the relative humidity rH of the dry room, which is determined by the dew point $T_D$ and the saturation vapor pressure $p_W^*$ ($T_{Dry\ room}$) of water depending on the temperature of the dry room: rH = $p_W^*$ ($T_D$)/$p_W^*$ ($T_{Dry\ room}$).

A reduction of the temperature from dryer to dry room is thus accompanied by an increase of the water activity of the gas phase, even if the dew point of the dry room and the dew point at the exit of dryer room are the same. Typical dew points of dry rooms in the battery production chain are around $T_D = -50$ °C.[2] Provided that the sorption equilibrium does not show any hysteresis, the electrode could be stored in the dry room instead of undergoing an energy intensive post drying process. This is illustrated in Figure 1.

Yet, previous investigations have shown that the electrodes do show hysteresis[3] and therefore need to be dried. Another advantage of high drying temperatures is the acceleration of the slow mass transport kinetics at low mass loadings. Kinetic effects will, however, not be addressed in this paper.

In order to remove the moisture cost efficiently, the process understanding needs to be improved by modeling. Although first efforts can be found in the literature,[4] the mechanisms of heat and mass transfer of water in electrodes for Li ion batteries are not completely understood. Of particular interest is the anode, as it contributes the most moisture to the cell.[4] Especially, waterborne binder systems play a key role.[3,5,6]

Concerning hysteresis in the sorption behavior of water in the electrodes for Li ion batteries, three challenges need to be addressed. First, relevant mechanisms that cause hysteresis of

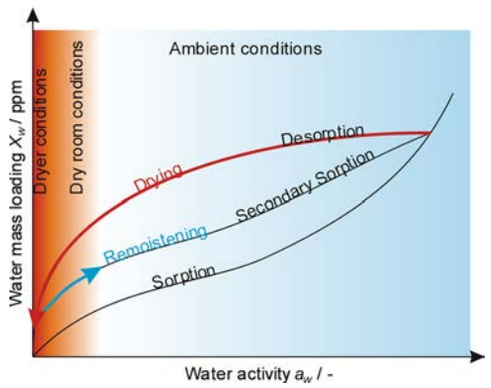


**Figure 1.** Schematic representation of the post drying process. The drying process starts at high water activity, wherefore the activity is reduced and the layer is dried. Because of the decrease in the temperature after the drying process, the electrode starts to resorb.

moisture sorption in the components of a Li ion battery need to be identified. Second, sorption/desorption and hysteresis scanning loops need to be distinguished. Between drying and post drying, the electrodes undergo further process steps. Thus, the course of desorption is unlikely to follow the whole path of the primary desorption isotherm but starts at a fluctuating relative humidity instead. This is why the desorption isotherm needs to be modeled depending on the sorption isotherm. Third, Figure 1 displays that an unwanted remoistening takes place during further cell processing because of an increase of water activity. A modeling of the secondary sorption isotherm depending on the primary sorption and desorption needs to be found. Provided that the electrodes are dried to a very low moisture content in the post drying process, remoistening runs on the primary sorption isotherm.

The phenomenon of hysteresis in adsorption/absorption and desorption in general has long been observed in water sorption[5,6] and an explanation for the hysteresis behavior has been sought.[7,8] Over the years, various theories have been employed to explain hysteresis. It is particularly difficult to evaluate the predominant mechanism in the sorption of moisture in battery electrodes, as a whole variety of different electrodes with different active materials, structure, and material composition is reported in the literature. For carbon electrode materials, graphite is deployed just like diamond or carbon nanotubes.[9] Besides, surface modifications or carbon composite electrodes are reported, for example, to address a volume change during (de)lithiation.[10,11] Chen et al. reported a new strategy to wrap Ni incorporated and N doped carbon nanotube arrays on porous Si and received a high reversible capacity as well as an excellent cycling stability.[12]

In the most common case for anodes of Li ion batteries, however, natural or synthetic graphite particles are employed, which are incorporated in a network of solvent or water based polymeric binders.[13,14] In the following, we focus on anodes that contain synthetic surface modified graphite particles, on which the moisture tends to adsorb, and water based polymeric binders, some of which rather show a volume uptake of the moisture and a high swelling behavior like that of carboxymethyl cellulose (CMC).

The following paragraphs will give a brief overview about the theories on adsorption and absorption.

**Adsorption.** An established model to describe the physical adsorption on solid sorbents is the BET equation named after Brunauer, Emmett, and Teller.[15]

$$X_i = \frac{X_\mathrm{m}\cdot k_\mathrm{BET}\cdot a_i}{(1-a_i)\cdot(1+(k_\mathrm{BET}-1)\cdot a_i)} \tag{1}$$

In the BET equation, $X_i$ is the loading of the sorbent, $a_i$ is the activity of the sorbate, and $k_\mathrm{BET}$ as well as $X_\mathrm{m}$ are parameters fitted to the measurement data.

The latter fit parameter of the BET equation, which describes the loading with a monolayer of a sorbate, also allows an experimental determination of the surface area of a sorbent in $m^2$ per g dry mass.

$$A_\mathrm{BET} = X_\mathrm{m}\cdot A_\mathrm{Adsorbate}\cdot\frac{N_\mathrm{A}}{\tilde{M}_\mathrm{Adsorptive}} \tag{2}$$

In eq 2, $N_\mathrm{A}$ is the Avogadro constant, $\tilde{M}_\mathrm{Adsorptive}$ is the molar mass of the adsorptive, and $A_\mathrm{Adsorbate}$ is the area occupied by an adsorbed sorbate molecule. For water, the literature value is given as $A_\mathrm{Water}$ = 12.5 Å$^2$.[16]

Furthermore, Brunauer et al. developed under some assumptions an extension of the model to material systems with a finite number of adsorbate layers and isotherms of different shapes, which is displayed in eq 3.[17,18]

$$X_i = \frac{X_\mathrm{m}\cdot k_\mathrm{BET}\cdot a_i}{(1-a_i)}\cdot \frac{1+\left(n\cdot\frac{g}{2}-n\right)\cdot a_i^{\,n-1}-(n\cdot g-n+1)\cdot a_i^{\,n}+\left(n\cdot\frac{g}{2}\right)\cdot a_i^{\,n+1}}{1+(k_\mathrm{BET}-1)\cdot a_i+\left(k_\mathrm{BET}\cdot\frac{g}{2}-k_\mathrm{BET}\right)\cdot a_i^{\,n}-\left(k_\mathrm{BET}\cdot\frac{g}{2}\right)\cdot a_i^{\,n+1}} \tag{3}$$

In eq 3, $(2n-1)$ is the number of layers of adsorbate that can fit in the walls of a pore. Moreover, $g$ is an additional temperature dependent fit parameter that is associated with the heat of adsorption in the last layer of the adsorbate.[17,18]

The temperature dependence of the fit parameters $g$ and $k_\mathrm{BET}$ can be presented in the following form

$$k_\mathrm{BET} = \exp\left(\frac{E}{\tilde{R}\cdot T}\right); \qquad g = \exp\left(\frac{Q}{\tilde{R}\cdot T}\right) \tag{4}$$

In eq 4, $E$ is the difference of the heat of adsorption in the first adsorbed layer and the heat of liquefaction. $Q$ is the difference of the heat of adsorption in the last adsorbed layer and the heat of liquefaction.

In the case of physical adsorption on solid sorbents, capillary condensation has been identified as the cause of hysteresis for many material systems. Various mechanisms were considered to explain the observation in detail, such as an incomplete wetting of pores during adsorption, ink bottle shaped pores, or a delay in the formation of the meniscus in the capillaries.[19,20] Cohan described how the partial pressures at which adsorption ($p_\mathrm{A}$) and desorption ($p_\mathrm{D}$) take place behave in a cylindrical pore with open ends.[18] He stated that these considerations also apply to closed capillaries with constrictions.[20]

$$\left(\frac{p_\mathrm{A}}{p^*(T)}\right)^{n_\mathrm{Cohan}} = \frac{p_\mathrm{D}}{p^*(T)} \tag{5}$$

In this equation, $p_\mathrm{A}$ is the partial pressure of adsorption, $p_\mathrm{D}$ is the partial pressure of desorption, and $p^*(T)$ is the saturation vapor pressure at a given temperature $T$. The exponent $n_\mathrm{Cohan}$ equals 2, if the corresponding requirements

of an ideal wetting behavior in a cylindrical or cylindrical constricted pore are fulfilled.[18,19]

In his model conception of capillary condensation, Cohan does not consider the pore structure or the pore network and regards only single cylindrical pores. In view of recent literature, Cohan's model is thought to be an over simplification.[21] Nevertheless, for some material systems, it provides a straightforward way to determine the primary desorption from the adsorption isotherm.

The exact form of hysteresis of adsorption exists in various shapes. The International Union of Pure and Applied Chemistry (IUPAC) has identified several different types of adsorption hysteresis loops depending on the pore and particle structure. A narrow pore size distribution between equal sized particles shows a different hysteresis form than the slit like pores between platelet shaped particles.[22,23]

With every form of hysteresis, the so called low pressure or open hysteresis may occur, meaning that hysteresis may be observed at the lowest attainable pressures.[22] Although an open hysteresis can also be enabled by chemisorption,[24] it is in case of physisorption associated with the swelling of a nonrigid pore structure or with the irreversible uptake of molecules in the pores of approximately the same width as that of the adsorbate molecule.[20,22] Moreover, the presence of permanent gases is also thought to be a reason for the irreversibility of adsorption.[20] Furthermore, an intercalation of polar molecules accompanied by the expansion and contraction of a sorbent might result in hysteresis over the complete range of activity, which has been observed during the sorption of polar sorbates in montmorillonite clays.[21,25]

Even though capillary condensation is unlikely to be the only hysteresis mechanism involved, it will play a role during sorption in the materials inside the electrode of a Li ion battery.

**Absorption.** A considerable amount of moisture in typical graphite anodes is, however, not adsorbed on the particles but absorbed in the binder CMC.[3] This cellulosic binder is a derivative of cellulose. In the anodes for Li ion batteries, usually its sodium salt is employed.

Cellulose is a material that has been extensively studied by researchers in the field of drying of wood. As there is not even agreement in the literature on the explanation of hysteresis in the sorption of water in cellulose, the description of hysteresis in whole electrode structures is even more complex.

Although different results have been acquired in the latest years,[26] early considerations assume a superposition of several mechanisms as a reason for sorption in cellulosic materials. Kollmann suggests that a saturation of hydroxyl groups occurs at low activities following a theory proposed by Urquhart.[27] He assumes that hysteresis is observed as unsaturated hydroxyl groups try to saturate each other during drying and are no longer available for the sorption of water molecules during sorption. This mechanism is succeeded by capillary condensation in the range of higher activities.[28] The idea of superimposing several processes in order to explain hysteresis in the sorption of water in cellulosic materials has remained to this day.[29,30] In addition to this, some recent studies attribute the hysteresis behavior in cellulosic materials only to capillary condensation,[31,32] whereas other studies relate hysteresis to structural changes when their glass transition temperature is exceeded.[33]

The latter follows the theory developed by Vrentas and Vrentas.[34,35] They explained the hysteresis behavior of the sorption of a solvent in polymers with structural changes because of an exceeding glass transition temperature of mixtures of solvents and polymers and used a modified Flory–Huggins approach in order to model the sorption isotherms.[36]

$$a_i = \phi_i \cdot \exp((1 - \phi_i) + \chi_{i,j}(1 - \phi_i)^2 + k \cdot F) \tag{6}$$

In this equation, $a_i$ is the activity of the solvent, $\phi_i$ is the volume fraction of the solvent, $\chi_{i,j}$ is the Flory–Huggins interaction parameter, and $F$ is defined by eq 7. The parameter $k$ equals 1 in case of absorption and deviates from 1 in case of desorption according to eq 9.[33,36]

$$F = \frac{\tilde{M}_i \cdot (1 - x_i)^2 \cdot (c_{p,S} - c_{p,S,g})}{\tilde{R} \cdot T} \left( \frac{dT_{gm}}{dx_i} \right) \left( \frac{T}{T_{gm}} - 1 \right)$$
$$T < T_{gm} \tag{7}$$

In eq 7, $\tilde{M}_i$ is the molar mass of the solvent, $x_i$ is the mass fraction of the solvent, $c_{p,S}$ and $c_{p,S,g}$ are the heat capacities of the polymer and the polymer in the glassy state, respectively, and $T_{gm}$ is the glass transition temperature of the mixture of the polymer and solvent. A correlation for the concentration dependent glass transition from the glass transition temperatures $T_{gi}$ and $T_{gj}$ of two materials is given in the equation by Fox.[37]

$$T_{gm} = \left( \frac{x_i}{T_{gi}} + \frac{(1 - x_i)}{T_{gj}} \right)^{-1} \tag{8}$$

If $T > T_{gm}$, $F$ equals zero. In this case, eq 6 represents the Flory–Huggins approach. The rate of change of $T_{gm}$ with a change in penetrant mass fraction can be obtained from the study of Pierlot.[38]

According to the model by Vrentas and Vrentas, the parameter $k$ can be calculated as follows

$$k = \frac{(T_D - T_{g2}) - T_D \cdot \ln\left(\frac{T_D}{T_{g2}}\right)}{(T - T_{g2}) - T \cdot \ln\left(\frac{T}{T_{g2}}\right)} \tag{9}$$

The fit parameter $T_D$ should not be confused with the dew point and represents, according to the model, a temperature which produces the same structure for an absorption sample which is equivalent to the desorption structure at temperature $T$. It can be adapted to measurement data, and $T_{g2}$ is the glass transition temperature of the polymer.[33]

Salmén and Larsson showed experimentally that hysteresis of chemically modified cellulosic materials varies with its softening behavior.[34] Hill and Beck were the first to apply the theory to their experimental results of the sorption of water in cellulose.[33]

By contrast, instead of eq 6, variations of the BET equation are employed to describe the primary sorption of water in cellulosic materials, especially in the literature about food processing technology.[39]

Regardless of the predominant mechanism for hysteresis, neither of the models of sorption isotherms mentioned here are able to predict hysteresis loops. Still, a way to describe a

secondary desorption from the sorption and desorption isotherms needs to be found.

In the literature about the adsorption on solid sorbents, this is done by applying the density functional theory.[32,40] A more straightforward semiempirical approach is proposed by Zhang et al.,[41] who considered a model suggested by Mualem.[42,43]

Though originally having been derived for the theory of capillary condensation, the equation proposed by Zhang et al. primarily mediates between the given adsorption/absorption and desorption isotherms. We propose a different empirical equation, following a similar approach, in order to describe the hysteresis behavior in electrodes for Li ion batteries.

During post drying of the electrodes, desorption occurs from the upper inflection point of the isotherm $X_U$ until the course of the primary desorption branch is reached. Consequently, the desorption loops with loading $X_{Des}$ are located between the primary sorption $X_{1.Sorp}$ and desorption $X_{1.Des}$ and can be described by eq 10.

$$X_{Des} = X_{1.Des} + (X_{1.Sorp} - X_{1.Des}) \cdot \left( \frac{X_{1.Sorp}}{X_U} \right)^{n_{Des}} \quad (10)$$

At high activities, the loading approaches the value of the primary sorption isotherm, whereas it approaches the value of the primary desorption isotherm for low activities.

The only parameter in this equation for the secondary desorption branch, which is not part of the modeling of the primary sorption or desorption, is the parameter $n_{Des}$. Empirical investigations show that $n_{Des} = 2$ is in good agreement with the experimental results.

## EXPERIMENTAL SECTION

In this paper, graphite anodes used in Li ion batteries were investigated consisting of graphite particles, carbon black as the conductive additive, and Na CMC as well as styrene butadiene rubber (SBR) as binders. Details about the materials and the experimental setups can be found in a former publication.[3] Table 1 summarizes the latter.

**Table 1. Overview of Experimental Setups**

| | method 1 | method 2 | method 3 |
|---|---|---|---|
| measurement setup | magnetic suspension balance | magnetic suspension balance | hydrosorb |
| gas phase | saturated gas flow | pure vapor | pure vapor |
| measurement principle | gravimetric | gravimetric | pressure |

Methods 1 and 2 are gravimetric measurement methods with a high resolution at sufficient sample masses and differ in the adjustment of the gas phase activity. Method 1 is operated at atmospheric pressure, and the dew point of the gas phase is adjusted by mixing a dry and a saturated gas flow, providing an opportunity to adjust low activities at low temperatures. Results of the measurements are compared to that of method 3, an acknowledged standard device for sorption isotherms.

In contrast to previous investigations, however, the drying temperature was decreased to $T = 90$ °C in all setups to prevent the binders from being damaged. Frequent repetition of experiments or excessively long drying times lead to changes in the phase equilibrium of the anode, which may be attributable to material changes in the binder when using high temperatures over long periods.

Measurements of the glass transition temperature were done by differential scanning calorimetry with DSC 204 from Netzsch.

## RESULTS AND DISCUSSION

It has been shown previously that the anode of a Li ion battery shows hysteresis in its sorption equilibrium.[3] The aim of this paper is to further evaluate this hysteresis behavior of anodes for Li ion batteries.

Graphite represents the biggest mass fraction among the materials in the anode of the Li ion battery. Its sorption isotherm represents most likely type IV from the IUPAC classification, and its hysteresis behavior at a temperature of $T = 30$ °C is displayed in Figure 2.

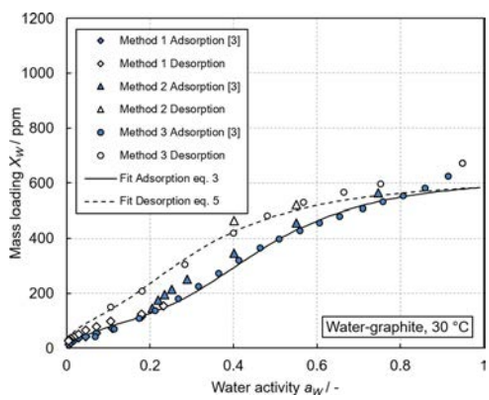


**Figure 2.** Hysteresis behavior of the sorption of water on graphite particles at $T = 30$ °C measured by three different experimental setups. Measurement values were fitted by using eq 3 for adsorption and eq 5 for desorption. Values of the adsorption isotherm are taken from a former publication.[3]

Graphite shows hysteresis in its phase equilibrium. The reason for hysteresis is assumed to be capillary condensation. The measurement data were fitted by using eq 3 for adsorption and eq 5 for desorption. The fit parameters are presented in Table 2. Deviations between measurement and model are visible in the range of the highest activity, as the model cannot reproduce the exact course of the entire isotherm. For the post drying process, this range of activity plays a minor role.

**Table 2. Fit Parameters for the Adsorption and Desorption of Water in Graphite**

| | $E$/J mol$^{-1}$ | $X_m$/ppm | $n$/- | $Q$/J mol$^{-1}$ | $n_{Cohan}$ |
|---|---|---|---|---|---|
| 1. adsorption | 6000 | 125 | 5 | 10,000 | |
| 1. desorption | 6000 | 125 | 5 | 10,000 | 1.5 |

The course of hysteresis reminds most of type H3 according to the IUPAC classification, which is associated with plate like particles.[22] This plate like structure can be confirmed from SEM images. Based on this, a possible model concept of water adsorption in the graphite particles is displayed in Figure 3.

Just like graphite, carbon black also shows hysteresis in its phase equilibrium. Figure 4 presents the measurement data, which remind of a type V isotherm according to the IUPAC classification that is associated with weak interactions between the sorbate and sorbent.[17]

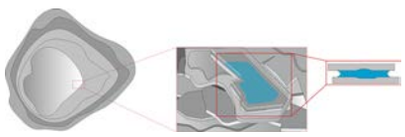

**Figure 3.** Possible model concept of water adsorption on the graphite particles. The particles exhibit a plate like structure that causes slit like pores in which water adsorbs.

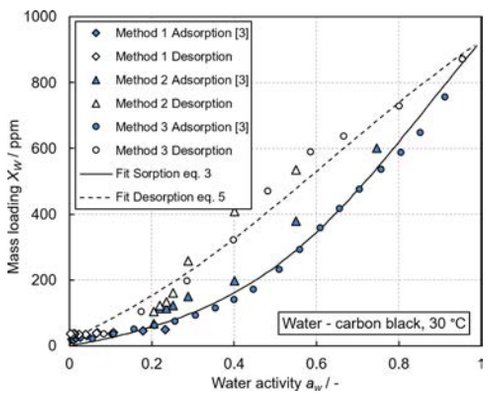


**Figure 4.** Hysteresis behavior of the sorption of water on carbon black particles at $T$ = 30 °C measured with three different setups. Measurement values were fitted by using eq 3 for adsorption and eq 5 for desorption. Values of the adsorption isotherm are taken from a former publication.[3]

The measurement data of the adsorption of water on carbon black were again fitted by using eq 3 for adsorption and eq 5 for desorption isotherms. Deviations are visible in the desorption branch, especially at low activities. The corresponding fit parameters are presented in Table 3.

**Table 3. Fit Parameters for the Adsorption and Desorption of Water in Carbon Black**

| | $E$/J mol$^{-1}$ | $X_m$/ppm | $n$/- | $Q$/J mol$^{-1}$ | $n_{Cohan}$ |
|---|---|---|---|---|---|
| 1. adsorption | 800 | 298 | 7 | 50 | |
| 1. desorption | 800 | 298 | 7 | 50 | 1.7 |

By and large, graphite and especially carbon black do not contribute to the sorption equilibrium of the anode with water to a large extent. By contrast, the binder CMC is mainly responsible for the water uptake in the anode.[3] Therefore, this binder has been tested for its hysteresis behavior.

An estimation of the inner surface or the pore volume, respectively, can be done by Argon sorption at $T$ = 87 K. The surface area of CMC particles determined from experiments accounted for a low value of $A_{BET,CMC}$ = 1.5 m$^2$/g.

Entirely different are the results from the experiments with water sorption and desorption, which are displayed in Figure 5. Films of CMC take up a huge amount of water. Moreover, the phase equilibrium of water in CMC is temperature dependent and exhibits hysteresis, which is also temperature dependent. At $T$ = 30 °C, hysteresis is quite distinct, whereas it almost disappears at $T$ = 90 °C. In Figure 5, the experimental values are compared to the model developed by Vrentas and Vrentas.

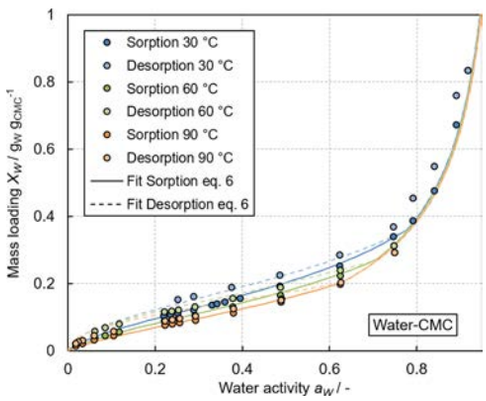


**Figure 5.** Hysteresis of water sorption in a layer of CMC at different temperatures and compared to the desorption model of eq 6. Measurement values were recorded using method 2.

Figure 5 shows that the model by Vrentas and Vrentas can describe the hysteresis behavior. Deviations emerge especially in the desorption at high activities and high temperatures. The former might be explained by additional capillary condensation. In the post drying process, though, values at high activities play a minor role. An improved adaption for higher temperatures might succeed by a different temperature dependence of the parameter $k$ in eq 9 from the fit parameter $T_D$.

The model requires a set of fit parameters which are given in Table 4. The glass transition temperature of pure water was taken from the literature as $T_{g,w}$ = 135 K.[44]

**Table 4. Fit Parameters of Hysteresis of Water Sorption in CMC**

| | $\Delta c_p$/J kg$^{-1}$ K$^{-1}$ | $T_{g,CMC}$/K- | $\chi$/- | $T_D$/K |
|---|---|---|---|---|
| 1. sorption | 380 | 550 | 0.3 | |
| 1. desorption | 380 | 550 | 0.3 | 220 |

The validity of two of these fit parameters, $T_{gm}$ and $\Delta c_p$, was verified by measurements with differential scanning calorimetry (DSC). For this purpose, CMC particles were loaded with moisture at different water activities. In DSC measurements, the glass transition temperature is visualized by a step.[45] Yet, not all samples showed a very pronounced step. The results are displayed in Figure 6 and compared to the used model from eq 8 given by Fox. In addition, available data from the literature for the glass transition temperature of cellulose with varying water content are displayed.[46,47]

In Figure 6, the measured data for CMC are in decent accordance to the used fit parameters and the model by Fox.[37] The glass transition temperature from the fit therefore seems to be in a reasonable range.

With DSC measurements, the heat capacity can also be determined. The difference in heat capacity at the step of glass transition turned out to be in the range of $\Delta c_p$ = 200 J/(kg K), which is lower but in the same order of magnitude as the fit parameter from Table 4. A reduction of the fit parameter, however, results in a flattening of the isotherms at low activities.

In conclusion, modeling the primary sorption and desorption isotherms of the phase equilibrium of water in CMC is reduced to only two unknown fit parameters $\chi_{i,j}$ and $T_D$.

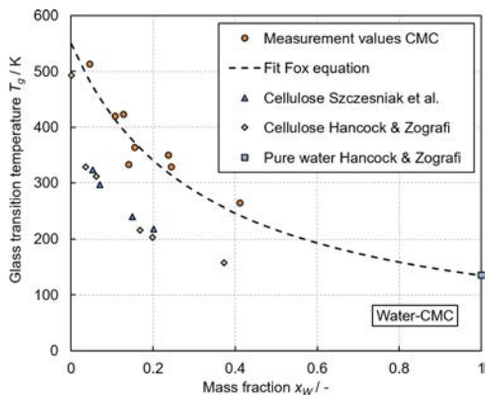


**Figure 6.** Glass transition temperature of CMC loaded with water as a function of the water content. Measurement values are compared to the model by Fox[37] and values from the literature from cellulose.[46,47]

In the production process of electrodes for Li ion batteries, it is particularly important for the description of the phase equilibrium to also be able to describe secondary desorption isotherms. Thus, the moisture content during varying conditions in the production process can be reproduced.

In Figure 7, measurement values of scanning hysteresis loops at $T$ = 30 °C are compared to the model description from eq 10.

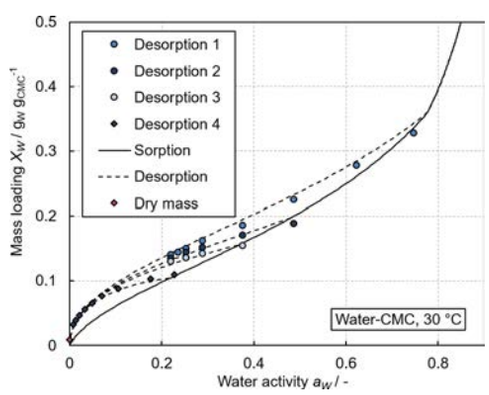


**Figure 7.** Hysteresis scanning loops of the sorption of water in a layer of CMC at $T$ = 30 °C. Measurement values were recorded using methods 1 (diamonds) and 2 (circles) and are compared to the model from eq 10. Also, the measurement value is marked, which was recorded after the desorption at $T$ = 30 °C and the dew point of the dry gas flow.

Figure 7 shows that the measurement values approach the primary desorption isotherm at lower activities. There is a decent accordance of the scanning hysteresis loops to their model description. Furthermore, the measurement value is marked, which was recorded after desorption at $T$ = 30 °C and the dew point of the dry gas flow. With thick layers of CMC, the decrease in mass at particularly low dew points becomes extremely slow. At low temperatures, the thick layers have not reached their equilibrium after days. If the material system shows an open hysteresis cannot be answered conclusively from this measurement. The low dew point of the dry gas stream, which is below the measurement range of the chilled mirror hygrometer, as well as kinetic effects can affect the deviations of the measurement and the exact equilibrium value.

The other binder, SBR, shows a more pronounced glass transition in DSC measurements. The experiments covered a range of activity from almost zero to $a_W$ = 0.32. However, the glass transition temperature of dry and moisture loaded SBR was below room temperature in all experiments, suggesting that no hysteresis would appear, according to the model by Vrentas and Vrentas, assuming the absorption of water in a film of SBR. The data of the measurement are displayed in Figure 8.

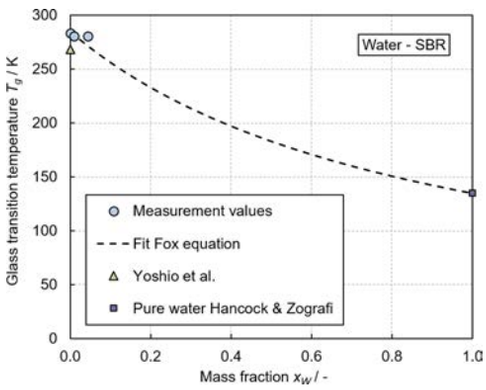


**Figure 8.** Glass transition temperature of SBR loaded with water, measured with DSC, as a function of the water content. Measurement values are compared to a fit of the equation by Fox[37] as well as a value from the literature with a similar SBR.[48]

In agreement with these considerations and DSC measure ments, hysteresis in the phase equilibrium of water in films made of SBR dispersion, which is displayed in Figure 9, could not be detected between $T$ = 30 °C and $T$ = 90 °C. However, there are indications that adsorption also plays a role in addition to absorption.

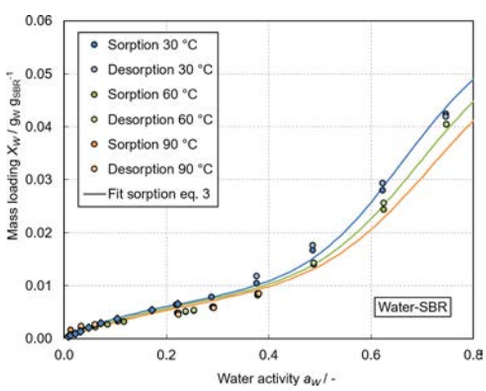


**Figure 9.** Phase equilibrium of the sorption of water in a film made of SBR particles. Measurement values at three different temperatures measured with two different setups, method 1 (diamonds) and 2 (circles), are compared to the fit from eq 3.

Although microscope images of the films suggest a complete film formation of the particles and therefore a volume uptake by the film, the surface area determined from the phase equilibrium according to eq 2 results in a value of around $A_{BET}$ = 30 $m^2/g$, which is quite similar to a value obtained assuming a close packing of SBR particles. Even though absorption particularly at a higher range of water activity is probable, it is presumed that the adsorption of water on and in between the SBR particles predominates for

the range of low water activity. In this range, which is especially important for the post drying process, measurement values, as shown in Figure 9, can be described by a fit from eq 3. The required density of SBR for the calculation of the surface area of a close packing was taken as $\rho_{SBR}$ = 1040 kg/m$^3$ from the manufacturer information, which agrees with the values from the literature.[49] The diameter of the SBR particles is in the range of $d_{SBR}$ = 150 nm.

As it has already been pointed out, Figure 9 shows the absence of hysteresis in the phase equilibrium with water in the considered temperature and concentration ranges. Deviations between sorption and desorption are rather attributable to measurement inaccuracies. The fit parameters according to eq 3 are given in Table 5. A fit from Flory–Huggins, displayed in eq 6, would be particularly suitable to fit the range of high activity.

**Table 5. Fit Parameters for the Sorption Equilibrium of Water in SBR According to eq 3**

| | $E$/J mol$^{-1}$ | $X_m$/kg kg$^{-1}$ | $n$/- | $Q$/J mol$^{-1}$ |
|---|---|---|---|---|
| sorption | 5241 | 0.00725 | 9 | 11,045 |

Just as the binder CMC, the anode shows a temperature dependent sorption equilibrium. It also has hysteresis, which is additionally temperature dependent. This is depicted in Figure 10.

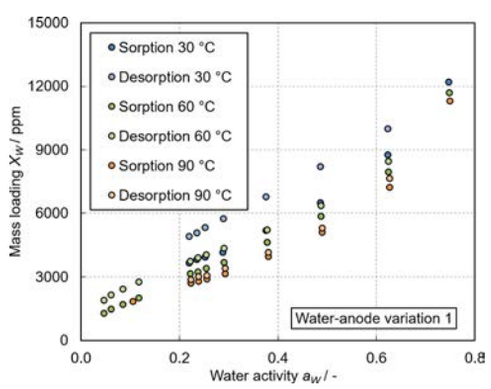


**Figure 10.** Hysteresis behavior of water sorption in an anode at three different temperatures. The sorption equilibrium and hysteresis are temperature dependent. Measurement values were recorded using method 2.

The width of hysteresis decreases with an increasing temperature. The phase equilibrium shows a distinct similarity to the equilibrium of its binder CMC. The comparison of the equilibrium of the anode to the found models of the sorption equilibria of its materials is therefore a logical step. In Figure 11, the measurement values at $T$ = 60 °C from Figure 10 are compared to the mass weighted addition of the equilibria of the materials of the anode. The equilibrium of the binder CMC is described by the parameters from Table 4, the equilibria of the particles with parameters from Tables 2 and 3, and the equilibrium with SBR from Table 5. The advantage of superimposing the equilibria of the materials to describe the equilibrium of the electrode takes effect as soon as changes in the material composition of the electrodes are carried out.

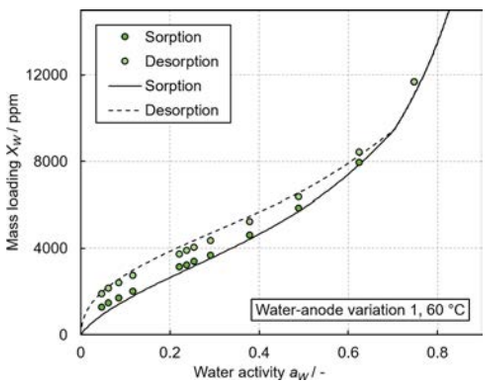


**Figure 11.** Hysteresis behavior of the sorption of water in an anode at 60 °C. Measurement data are compared to the addition of its materials. CMC is described by the model by Vrentas and Vrentas, with fit parameters from Table 4; the data of the equilibria of the particles are taken from Tables 2 and 3 and those of the equilibrium with SBR from Table 5.

Figure 11 shows a decent accordance between the measurement values and the addition of the equilibria of the materials. Yet, the model description of desorption from Figure 11 only represents a primary desorption isotherm. Scanning isotherm loops are particularly important when describing the moisture desorption in the post drying process of electrodes for lithium ion batteries and the moisture loading in the entire electrode production chain.

When scanning the hysteresis loops, it becomes visible that individual desorption branches approach the primary desorption curve. More information is provided in the Supporting Information in Figure S12. Curves of mass loading of moisture in the electrode production also run on hysteresis loops of the phase equilibrium after coating and drying.

The applicability of this model is not confined to this specific anode. An anode with a different binder content has also been investigated. A secondary desorption isotherm as well as the corresponding model is also displayed in the Supporting Information in Figure S13.

## CONCLUSIONS

The sorption equilibrium of water in a graphite anode of a Li ion battery has been investigated. It shows hysteresis, which is caused by different mechanisms. While capillary condensation is assumed to cause hysteresis in the particles, graphite and carbon black, exceeding the glass transition temperature is suspected to cause hysteresis in the sorption equilibrium with the binder Na CMC.

The relevance of this hysteresis in the sorption equilibrium for the residual moisture content in the production process of electrodes for Li ion batteries is pointed out. In order to achieve a low residual moisture content, hysteresis needs to be overcome. As especially the binder Na CMC shows a low pressure hysteresis, low activities need to be attained in the post drying process.

It was discovered that the experimental data of the hysteresis loops approach a curve that can be described from the equilibria of the materials of the anode for a wide range of water activities and temperatures. Individual hysteresis loops are modeled based on the data from the sorption and desorption isotherms. This approach to describe the desorption isotherm is required in order to model the

post drying process of electrodes for Li ion batteries and their moisture loading in the electrode production chain. With the help of these models, it is possible to determine the equilibrium moisture loading, which is going to adjust in the electrodes, as long as the electrodes are given enough time or the diffusion of water in the anode is rapid enough.

## AUTHOR INFORMATION


### Corresponding Author

**Jochen C. Eser** − *Institute for Thermal Process Engineering—Thin Film Technology, Karlsruhe Institute of Technology, 76131 Karlsruhe, Germany;* orcid.org/0000 0002 7393 5427; Email: jochen.eser@kit.edu

### Authors

**Birthe Deichmann** − *Institute for Thermal Process Engineering—Thin Film Technology, Karlsruhe Institute of Technology, 76131 Karlsruhe, Germany*

**Tobias Wirsching** − *Institute for Thermal Process Engineering—Thin Film Technology, Karlsruhe Institute of Technology, 76131 Karlsruhe, Germany*

**Peter G. Weidler** − *Institute of Functional Interfaces, Karlsruhe Institute of Technology, 76344 Eggenstein Leopoldshafen, Germany*

**Philip Scharfer** − *Institute for Thermal Process Engineering—Thin Film Technology, Karlsruhe Institute of Technology, 76131 Karlsruhe, Germany*

**Wilhelm Schabel** − *Institute for Thermal Process Engineering—Thin Film Technology, Karlsruhe Institute of Technology, 76131 Karlsruhe, Germany*

Complete contact information is available at: https://pubs.acs.org/10.1021/acs.langmuir.0c00704


### Author Contributions

The manuscript was written through contributions of all authors. All authors have given approval to the final version of the manuscript.


### Funding

The authors thank the BMBF for the financial support within the ProZell Cluster Project Roll It (03XP0080A).


### Notes

The authors declare no competing financial interest.


## ACKNOWLEDGMENTS

The authors thank Andreas Roth, Gerrit Schöne and Sabrina Herberger from KIT TVT for support in experiments.


## ABBREVIATIONS

CMC, carboxymethyl cellulose; DSC, differential scanning calorimetry; IUPAC, International Union of Pure and Applied Chemistry; SBR, styrene butadiene rubber

## REFERENCES


(1) Schunemann, J. H.; Dreger, H.; Bockholt, H.; Kwade, A. Smart Electrode Processing for Battery Cost Reduction. *ECS Trans.* **2016**, *73*, 153−159.

(2) Kaiser, J.; Wenzel, V.; Nirschl, H.; Bitsch, B.; Willenbacher, N.; Baunach, M.; Schmitt, M.; Jaiser, S.; Scharfer, P.; Schabel, W. Process and product development of electrodes for lithium ion cells. *Chem. Ing. Tech.* **2014**, *86*, 695−706.

(3) Eser, J. C.; Wirsching, T.; Weidler, P. G.; Altvater, A.; Börnhorst, T.; Kumberg, J.; Schöne, G.; Müller, M.; Scharfer, P.; Schabel, W. Moisture adsorption behavior in anodes for Li ion batteries. *Energy Technol.* **2019**, *8*, 1801162.

(4) Stich, M.; Pandey, N.; Bund, A. Drying and moisture resorption behaviour of various electrode materials and separators for lithium ion batteries. *J. Power Sources* **2017**, *364*, 84−91.

(5) van Bemmelen, J. M. Die Absorption. Das Wasser in den Kolloïden, besonders in dem Gel der Kieselsäure. *Z. Anorg. Chem.* **1897**, *13*, 233−356.

(6) Zsigmondy, R. Über die Struktur des Gels der Kieselsäure. Theorie der Entwässerung. *Z. Anorg. Allg. Chem.* **1911**, *71*, 356−377.

(7) Foster, A. G. The Sorption of Vapours by Ferric Oxide Gel. I. Aliphatic Alcohols. *Proc. R. Soc. A* **1934**, *147*, 128−140.

(8) McBain, J. W. An explanation of hysteresis in the hydration and dehydration of gels. *J. Am. Chem. Soc.* **1935**, *57*, 699−700.

(9) McCreery, R. L. Advanced carbon electrode materials for molecular electrochemistry. *Chem. Rev.* **2008**, *108*, 2646−2687.

(10) Yim, C. H.; Courtel, F. M.; Abu Lebdeh, Y. A high capacity silicon−graphite composite as anode for lithium ion batteries using low content amorphous silicon and compatible binders. *J. Mater. Chem. A* **2013**, *1*, 8234.

(11) Chae, S.; Choi, S. H.; Kim, N.; Sung, J.; Cho, J. Integration of Graphite and Silicon Anodes for the Commercialization of High Energy Lithium Ion Batteries. *Angew. Chem., Int. Ed. Engl.* **2020**, *59*, 110−135.

(12) Chen, M.; Jing, Q. S.; Sun, H. B.; Xu, J. Q.; Yuan, Z. Y.; Ren, J. T.; Ding, A. X.; Huang, Z. Y.; Dong, M. Y. Engineering the Core−Shell Structured NCNTs Ni 2 Si@Porous Si Composite with Robust Ni−Si Interfacial Bonding for High Performance Li Ion Batteries. *Langmuir* **2019**, *35*, 6321−6332.

(13) Jaiser, S.; Funk, L.; Baunach, M.; Scharfer, P.; Schabel, W. Experimental investigation into battery electrode surfaces: The distribution of liquid at the surface and the emptying of pores during drying. *J. Colloid Interface Sci.* **2017**, *494*, 22−31.

(14) Baunach, M.; Jaiser, S.; Schmelzle, S.; Nirschl, H.; Scharfer, P.; Schabel, W. Delamination behavior of lithium ion battery anodes: Influence of drying temperature during electrode processing. *Drying Technol.* **2015**, *34*, 462−473.

(15) Brunauer, S.; Emmett, P. H.; Teller, E. Adsorption of Gases in Multimolecular Layers. *J. Am. Chem. Soc.* **1938**, *60*, 309−319.

(16) Brunauer, S.; Kantro, D. L.; Weise, C. H. The surface energies of amorphous silica and hydrous amorphous silica. *Can. J. Chem.* **1956**, *34*, 1483−1496.

(17) Brunauer, S.; Deming, L. S.; Deming, W. E.; Teller, E. On a Theory of the van der Waals Adsorption of Gases. *J. Am. Chem. Soc.* **1940**, *62*, 1723−1732.

(18) Do, D. D. *Adsorption Analysis: Equilibria and Kinetics*, 1st ed.; Series on Chemical Engineering; Imperial College Press: London, 1998; Vol. 2.

(19) Cohan, L. H. Sorption Hysteresis and the Vapor Pressure of Concave Surfaces. *J. Am. Chem. Soc.* **1938**, *60*, 433−435.

(20) Cohan, L. H. Hysteresis and the Capillary Theory of Adsorption of Vapors. *J. Am. Chem. Soc.* **1944**, *66*, 98−105.

(21) Sing, K. S. W.; Williams, R. T. Physisorption Hysteresis Loops and the Characterization of Nanoporous Materials. *Adsorpt. Sci. Technol.* **2004**, *22*, 773−782.

(22) Sing, K. S. W. Reporting physisorption data for gas/solid systems with special reference to the determination of surface area and porosity (Provisional). *Pure Appl. Chem.* **1982**, *54*, 2201−2218.

(23) Thommes, M.; Kaneko, K.; Neimark, A. V.; Olivier, J. P.; Rodriguez Reinoso, F.; Rouquerol, J.; Sing, K. S. W. Physisorption of gases, with special reference to the evaluation of surface area and pore size distribution (IUPAC Technical Report). *Pure Appl. Chem.* **2015**, *87*, 1051−1069.
(24) Lowell, S.; Shields, J. E.; Thomas, M. A.; Thommes, M. *Characterization of Porous Solids and Powders: Surface Area*; Pore Size and Density; Springer Netherlands: Dordrecht, 2004; Vol. *16*.
(25) Barrer, R. M. Clay minerals as selective and shape selective sorbents. *Pure Appl. Chem.* **1989**, *61*, 1903−1912.
(26) Chen, M.; Coasne, B.; Guyer, R.; Derome, D.; Carmeliet, J. Role of hydrogen bonding in hysteresis observed in sorption induced swelling of soft nanoporous polymers. *Nat. Commun.* **2018**, *9*, 3507.
(27) Urquhart, A. R. 15 The Mechanism of the Adsorption of Water by Cotton. *J. Text. Inst., Trans.* **1929**, *20*, T125−T132.
(28) Kollmann, F. Sorption und Quellung des Holzes. *Naturwissenschaften* **1944**, *32*, 121−139.
(29) Fredriksson, M.; Thybring, E. E. Scanning or desorption isotherms?: Characterising sorption hysteresis of wood. *Cellulose* **2018**, *25*, 4477−4485.
(30) Shi, J.; Avramidis, S. Water sorption hysteresis in wood: I review and experimental patterns − geometric characteristics of scanning curves. *Holzforschung* **2017**, *71*, 307−316.
(31) Shi, J.; Avramidis, S. Water sorption hysteresis in wood: II mathematical modeling − functions beyond data fitting. *Holzfor schung* **2017**, *71*, 317−326.
(32) Shi, J.; Avramidis, S. Water sorption hysteresis in wood: III physical modeling by molecular simulation. *Holzforschung* **2017**, *71*, 733−741.
(33) Hill, C.; Beck, G. On the applicability of the Flory−Huggins and Vrentas models for describing the sorption isotherms of wood. *Int. Wood Prod. J.* **2017**, *8*, 50−55.
(34) Salmén, L.; Larsson, P. A. On the origin of sorption hysteresis in cellulosic materials. *Carbohydr. Polym.* **2018**, *182*, 15−20.
(35) Engelund, E. T.; Thygesen, L. G.; Svensson, S.; Hill, C. A. S. A critical discussion of the physics of wood−water interactions. *Wood Sci. Technol.* **2013**, *47*, 141−161.
(36) Vrentas, J. S.; Vrentas, C. M. Hysteresis Effects for Sorption in Glassy Polymers. *Macromolecules* **1996**, *29*, 4391−4396.
(37) Smith, L.; Schmitz, V. The effect of water on the glass transition temperature of poly(methyl methacrylate). *Polymer* **1988**, *29*, 1871−1878.
(38) Pierlot, A. P. Water in Wool. *Text. Res. J.* **1999**, *69*, 97−103.
(39) Torres, M. D.; Moreira, R.; Chenlo, F.; Vázquez, M. J. Water adsorption isotherms of carboxymethyl cellulose, guar, locust bean, tragacanth and xanthan gums. *Carbohydr. Polym.* **2012**, *89*, 592−598.
(40) Landers, J.; Gor, G. Y.; Neimark, A. V. Density functional theory methods for characterization of porous materials. *Colloid. Surface. Physicochem. Eng. Aspect.* **2013**, *437*, 3−32.
(41) Zhang, X.; Zillig, W.; Künzel, H. M.; Zhang, X.; Mitterer, C. Evaluation of moisture sorption models and modified Mualem model for prediction of desorption isotherm for wood materials. *Build. Environ.* **2015**, *92*, 387−395.
(42) Mualem, Y. Modified approach to capillary hysteresis based on a similarity hypothesis. *Water Resour. Res.* **1973**, *9*, 1324−1331.
(43) Mualem, Y. A conceptual model of hysteresis. *Water Resour. Res.* **1974**, *10*, 514−520.
(44) Hancock, B. C.; Zografi, G. The Use of Solution Theories for Predicting Water Vapor Absorption by Amorphous Pharmaceutical Solids: A Test of the Flory−Huggins and Vrentas Models. *Pharm. Res.* **1993**, *10*, 1262−1267.
(45) Schabel, W. Trocknung von Polymerfilmen. Ph.D. Thesis, Karlsruhe Institute of Technology, Karlsruhe, 2004.
(46) Hancock, B. C.; Zografi, G. The Relationship Between the Glass Transition Temperature and the Water Content of Amorphous Pharmaceutical Solids. *Pharm. Res.* **1994**, *11*, 471−477.
(47) Szcześniak, L.; Rachocki, A.; Tritt Goc, J. Glass transition temperature and thermal decomposition of cellulose powder. *Cellulose* **2008**, *15*, 445−451.
(48) Yoshio, M.; Brodd, R. J.; Kozawa, A. *Lithium Ion Batteries: Science and Technologies*; Springer: New York, NY, 2009.
(49) Bitsch, B.; Dittmann, J.; Schmitt, M.; Scharfer, P.; Schabel, W.; Willenbacher, N. A novel slurry concept for the fabrication of lithium ion battery electrodes with beneficial properties. *J. Power Sources* **2014**, *265*, 81−90.